

Electron-doping evolution of the low-energy spin excitations in the iron arsenide $\text{BaFe}_{2-x}\text{Ni}_x\text{As}_2$ superconductors

Miaoyin Wang,¹ Huiqian Luo,² Jun Zhao,¹ Chenglin Zhang,¹ Meng Wang,^{2,1} Karol Marty,³ Songxue Chi,⁴ Jeffrey W. Lynn,⁴ Astrid Schneidewind,^{5,6} Shiliang Li,^{2,*} and Pengcheng Dai^{1,2,3,†}

¹*Department of Physics and Astronomy, The University of Tennessee, Knoxville, Tennessee 37996-1200, USA*

²*Beijing National Laboratory for Condensed Matter Physics and Institute of Physics, Chinese Academy of Sciences, P. O. Box 603, Beijing 100190, China*

³*Neutron Scattering Science Division, Oak Ridge National Laboratory, Oak Ridge, Tennessee 37831-6393, USA*

⁴*NIST Center for Neutron Research, National Institute of Standards and Technology, Gaithersburg, MD 20899, USA*

⁵*Gemeinsame Forschergruppe HZB - TU Dresden,*

Helmholtz-Zentrum Berlin für Materialien und Energie, D-14109 Berlin, Germany

⁶*Forschungsneutronenquelle Heinz Maier-Leibnitz (FRM-II), TU München, D-85747 Garching, Germany*

We use elastic and inelastic neutron scattering to systematically investigate the evolution of the low-energy spin excitations of the iron arsenide superconductor $\text{BaFe}_{2-x}\text{Ni}_x\text{As}_2$ as a function of nickel doping x . In the undoped state, BaFe_2As_2 exhibits a tetragonal-to-orthorhombic structural phase transition and simultaneously develops a collinear antiferromagnetic (AF) order below $T_N = 143$ K. Upon electron-doping of $x = 0.075$ to induce bulk superconductivity with $T_c = 12.3$ K, the AF ordering temperature reduces to $T_N \approx 58$ K. We show that the appearance of bulk superconductivity in $\text{BaFe}_{1.925}\text{Ni}_{0.075}\text{As}_2$ coincides with a dispersive neutron spin resonance in the spin excitation spectra, and a reduction in the static ordered moment. For optimally doped $\text{BaFe}_{1.9}\text{Ni}_{0.1}\text{As}_2$ ($T_c = 20$ K) and overdoped $\text{BaFe}_{1.85}\text{Ni}_{0.15}\text{As}_2$ ($T_c = 15$ K) superconductors, the static AF long-range order is completely suppressed and the spin excitation spectra are dominated by a resonance and spin-gap at lower energies. We determine the electron-doping dependence of the neutron spin resonance and spin gap energies, and demonstrate that the three-dimensional nature of the resonance survives into the overdoped regime. If spin excitations are important for superconductivity, these results would suggest that the three-dimensional character of the electronic superconducting gaps are prevalent throughout the phase diagram, and may be critical for superconductivity in these materials.

PACS numbers: 74.25.Ha, 74.70.-b, 78.70.Nx

I. INTRODUCTION

An experimental determination of the doping evolution of the spin excitations in iron arsenide superconductors [1–4] is important for a comprehensive understanding of the role of magnetism in the superconductivity of these materials. Like high-transition temperature (high- T_c) copper oxides, the parent compounds of iron arsenide superconductors exhibit static antiferromagnetic (AF) long-range order with a collinear spin structure [5–8]. Although there is currently no consensus on a microscopic mechanism for superconductivity, spin excitations have been postulated by several theories to play a crucial role in the electron pairing and superconductivity of these materials [9–13]. In one class of unconventional microscopic theories for superconductivity, electron pairing in iron arsenide superconductors is mediated by quasiparticle excitations between sign reversed hole pockets around the Γ point and the electron Fermi pockets around the M point as shown in the inset of Fig. 1(a) [14]. If this is indeed the case, spin excitations in the superconducting state should have a collective mode called the neutron spin resonance, whose energy is at (or slightly less than) the addition of the hole and electron superconducting gap energies ($E = |\Delta(k+Q) + \Delta(k)|$), where Q is the AF ordering wavevector connecting the

hole and electron Fermi pockets at the Γ and M points, respectively) [15–18]. Although recent inelastic neutron scattering experiments have found the neutron spin resonance for different iron-based superconductors consistent with this picture [19–26], a surprising result has been that the mode in the optimally doped $\text{BaFe}_{1.9}\text{Ni}_{0.1}\text{As}_2$ ($T_c = 20$ K) has three-dimensional character with clear dispersion along the c -axis [21, 22], quite different from the two-dimensional nature of the resonance in copper oxide superconductors [27–32]. If spin excitations are important for superconductivity in iron-arsenides, it would be interesting to systematically investigate the doping evolution of the resonance in $\text{BaFe}_{2-x}\text{Ni}_x\text{As}_2$, and determine if the three-dimensional nature of the mode is a general phenomenon or specific only to the optimally doped materials. Furthermore, since spin waves in the AF ordered parent compounds of $(\text{Ba},\text{Sr},\text{Ca})\text{Fe}_2\text{As}_2$ have rather large anisotropy spin gaps at the AF zone center [33–38] and the optimally doped superconducting samples are generally gapless [20–22, 26], it would be important to see how spin waves in the parent compounds evolve as electrons are doped into the FeAs planes.

In this article, we report our inelastic neutron scattering studies of the low-energy spin excitations in electron-doped $\text{BaFe}_{2-x}\text{Ni}_x\text{As}_2$ with $x = 0.075, 0.15$ [Fig. 1(a)], and compare and contrast them with the spin excitations

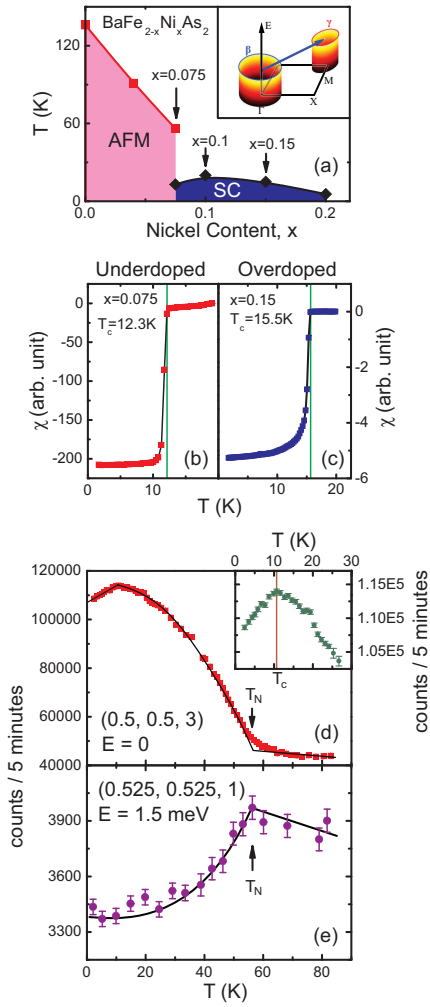


FIG. 1. (color online) (a) Electronic phase diagram of BaFe_{2-x}Ni_xAs₂ as determined from our previous [21, 22, 41] and current neutron scattering work. The inset shows schematic illustration of quasiparticle excitations from the hole pocket at the Γ point to the electron pocket at the M point as predicted by various theories [15–18]. (b,c) Temperature dependence of the Meissner and shielding signals on small crystals of BaFe_{1.925}Ni_{0.075}As₂ and BaFe_{1.85}Ni_{0.15}As₂. (d) Temperature dependence of the $Q = (0.5, 0.5, 3)$ magnetic Bragg peak in BaFe_{1.925}Ni_{0.075}As₂, showing a clear anomaly at T_N and T_c . The inset shows an expanded view of the $Q = (0.5, 0.5, 3)$ magnetic Bragg peak near T_c . (e) Temperature dependence of the quasi-elastic scattering at $E = 1.5$ meV and $Q = (0.525, 0.525, 1)$ shows a clear anomaly at $T_N = 58$ K.

observed at optimal doping and in the lightly/undoped regime. Before Ni-doping, BaFe₂As₂ exhibits simultaneous structural and magnetic phase transitions below $T_s = T_N = 143$ K, changing the crystal lattice symmetry from the high-temperature tetragonal to the low-temperature orthorhombic phase [7]. Upon doping electrons via either Co or Ni substitution for Fe, the structural and magnetic phase transitions are separated [39, 40]. For $x = 0.04$

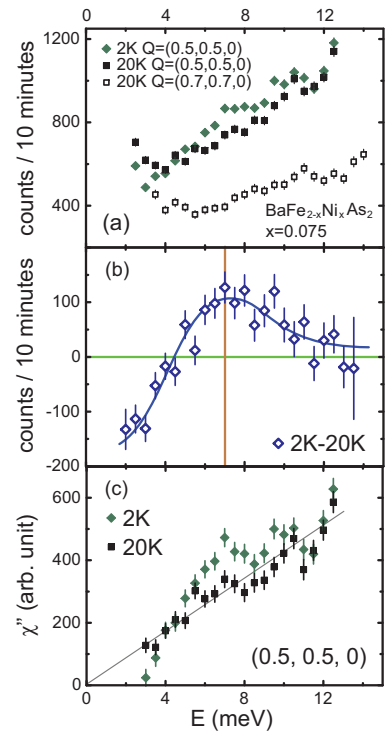


FIG. 2. (color online) (a) Energy scans at $Q = (0.5, 0.5, 0)$ (signal) and $Q = (0.7, 0.7, 0)$ (background) positions above and below T_c for BaFe_{1.925}Ni_{0.075}As₂. (b) The temperature difference plot (low temperature minus high temperature) in $S(Q, \omega)$ shows a clear neutron spin resonance at $E = 7$ meV below T_c . The solid line is a guide to the eye. (c) Estimation of the temperature dependence of the $\chi''(Q, \omega)$ above and below T_c , using background determined both from constant-energy scans and from constant- Q scans at background position.

Ni-doping, the structural and magnetic phase transition temperatures of BaFe_{1.96}Ni_{0.04}As₂ become near 97 K and 91 K, respectively [41]. In addition, three dimensional spin waves in BaFe₂As₂ change into quasi-two-dimensional spin excitations for BaFe_{1.96}Ni_{0.04}As₂ with no evidence for the neutron spin resonance [41] or bulk superconductivity [4]. By increasing the Ni-doping x to 0.075 to form BaFe_{1.925}Ni_{0.075}As₂ [Fig. 1(a)], bulk superconductivity appears at $T_c = 12.3$ K [Fig. 1(b)] and the Néel temperature of the material is now reduced to $T_N \approx 58$ K [Figs. 1(d) and 1(e)]. Our inelastic neutron scattering experiments show the presence of a three-dimensional neutron spin resonance with distinct energies at the AF wavevectors $Q = (0.5, 0.5, 0)$ and $(0.5, 0.5, 1)$, quite similar to that of the optimally doped BaFe_{1.9}Ni_{0.1}As₂ [21, 22]. The intensity gain of the mode below T_c is compensated by opening a pseudo spin gap at lower energies and reduction in the static AF order [see inset in Fig. 1(d)].

To study the doping evolution of the resonance, we

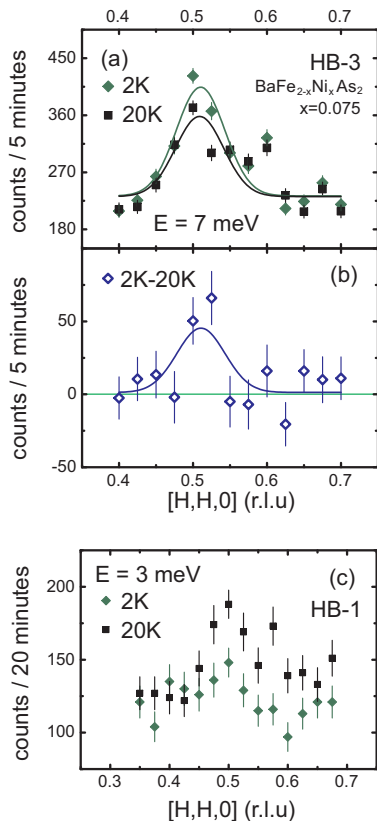


FIG. 3. (color online) (a) Constant-energy scans near the resonance energy ($E = 7$ meV) along the $(H, H, 0)$ direction across T_c for $\text{BaFe}_{1.925}\text{Ni}_{0.075}\text{As}_2$. The scattering clearly increases at the $Q = (0.5, 0.5, 0)$ below T_c . The small peak at $Q = (0.6, 0.6, 0)$ is spurious. (b) Temperature difference plot confirms the intensity gain at $Q = (0.5, 0.5, 0)$ below T_c . (c) Wave-vector scans at $E = 3$ meV. Here the scattering at $Q = (0.5, 0.5, 0)$ decreases below T_c but there is no spin gap at $E = 3$ meV.

also carried out inelastic neutron scattering experiments on overdoped $\text{BaFe}_{1.85}\text{Ni}_{0.15}\text{As}_2$ [$T_c = 15.5$ K, Fig. 1(c)] and found that the energy of the mode is approximately proportional to T_c . Our elastic neutron scattering measurements indicate that the static antiferromagnetism has been completely suppressed, while the neutron spin resonance in the superconducting state exhibits similar dispersion along the c -axis as the underdoped and optimally doped materials. This suggests that the three-dimensional nature of the resonance energy and its associated superconducting gap energy Δ are prevalent throughout the superconducting electronic phase diagram. These results can also provide information needed for calculating the electron-doping dependence of the AF coupling between the layers, and estimating the doping dependence of the superconducting gap energy.

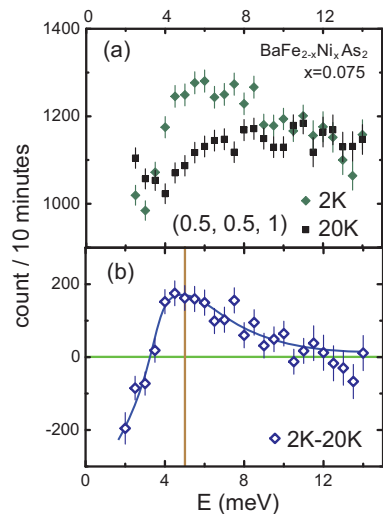


FIG. 4. (color online) (a) Constant- Q scans at $Q = (0.5, 0.5, 1)$ above and below T_c for $\text{BaFe}_{1.925}\text{Ni}_{0.075}\text{As}_2$. The scattering shows clear asymmetric enhancement around $E = 5$ meV below T_c . (b) Temperature difference plot reveals a neutron spin resonance at $E = 5$ meV, clearly below the energy of the mode at $Q = (0.5, 0.5, 0)$ as shown in Fig. 2.

II. EXPERIMENTAL DETAILS

In two recent inelastic neutron scattering experiments on underdoped $\text{BaFe}_{1.906}\text{Co}_{0.094}\text{As}_2$ ($T_c = 15$ K) [24] and $\text{BaFe}_{1.92}\text{Co}_{0.08}\text{As}_2$ ($T_c = 11$ K) [25], static AF order was found to coexist with superconductivity and cooling below T_c 's in these samples induced a weak neutron spin resonance in the magnetic excitation spectra at the expense of elastic magnetic scattering [24, 25]. For $\text{BaFe}_{2-x}\text{Ni}_x\text{As}_2$, bulk superconductivity appears only when $x \geq 0.05$ [4]. To compare the electronic phase diagram of $\text{BaFe}_{2-x}\text{Ni}_x\text{As}_2$ with Co-doped materials and see the effect of superconductivity on the spin excitations, we chose to study underdoped $\text{BaFe}_{1.925}\text{Ni}_{0.075}\text{As}_2$ (where Ni concentration is nominal) and overdoped $\text{BaFe}_{1.85}\text{Ni}_{0.15}\text{As}_2$ superconductors. The temperature dependence of the susceptibility in Figures 1(b) and 1(c) show T_c 's of 12.3 K and 15.5 K for $\text{BaFe}_{1.925}\text{Ni}_{0.075}\text{As}_2$ and $\text{BaFe}_{1.85}\text{Ni}_{0.15}\text{As}_2$, respectively, consistent with the overall electronic phase diagram from heat capacity measurements [4].

We grew single crystals of $\text{BaFe}_{2-x}\text{Ni}_x\text{As}_2$ with $x = 0.075, 0.15$ using the self-flux method [3]. Our neutron scattering experiments were carried out on the HB-3, HB-1 thermal triple-axis spectrometers at the high-flux-isotope reactor (HFIR), Oak Ridge National Laboratory [33]; the BT-7 thermal triple-axis spectrometer at the NIST Center for Neutron Research [22]; and the PANDA cold triple-axis spectrometer at the Forschungsneutronenquelle Heinz Maier-Leibnitz (FRM-II), TU München [21]. We defined the wave vector Q at (q_x, q_y, q_z) as

$(H, K, L) = (q_x a/2\pi, q_y b/2\pi, q_z c/2\pi)$ reciprocal lattice units (rlu) using the tetragonal nuclear unit cell, where $a = 3.89 \text{ \AA}$, $b = 3.89 \text{ \AA}$, and $c = 12.77 \text{ \AA}$. We co-aligned about 6 grams for each of the $x = 0.075, 0.15$ samples of $\text{BaFe}_{2-x}\text{Ni}_x\text{As}_2$ in the $[H, H, L]$ horizontal scattering plane, and put our samples inside either a closed cycle refrigerator or a liquid He cryostat.

For thermal triple-axis measurements on HB-1, HB-3, and BT-7, we used pyrolytic graphite (PG) as monochromator and analyzer with typical collimations of open- $40''$ -S- $40''$ - $120''$. The final neutron energy was chosen to be either $E_f = 13.5 \text{ meV}$ or $E_f = 14.7 \text{ meV}$ with a PG filter before the analyzer. For cold triple-axis measurements on PANDA, we chose final neutron energy of $E_f = 5.0 \text{ meV}$ with a cooled Be filter in front of the analyzer. We used both horizontal and vertical focusing PG monochromator and analyzer with no collimators. We also used a $E_f = 13.5 \text{ meV}$ setup with a PG filter in one of the PANDA measurements.

III. RESULTS AND DISCUSSIONS

We first describe our elastic and quasielastic neutron scattering results on the underdoped $\text{BaFe}_{1.925}\text{Ni}_{0.075}\text{As}_2$. Consistent with earlier results on underdoped $\text{BaFe}_{1.906}\text{Co}_{0.094}\text{As}_2$ [24] and $\text{BaFe}_{1.92}\text{Co}_{0.08}\text{As}_2$ [25], the AF structure of the $\text{BaFe}_{1.925}\text{Ni}_{0.075}\text{As}_2$ sample reported here is identical to the undoped parent compound but with a Néel $T_N \approx 58 \text{ K}$ [Fig. 1(c)]. The temperature dependence of the quasielastic scattering at $Q = (0.525, 0.525, 1)$ and $E = 1.5 \text{ meV}$ shows a clear kink below $\sim 58 \text{ K}$, thus confirming the Néel temperature of the system. The inset in Figure 1(d) shows the expanded temperature dependence of the AF Bragg peak intensity at $Q = (0.5, 0.5, 3)$. The scattering decreases with decreasing temperature at the onset of T_c , suggesting that the static moment competes with superconductivity similar to the Co-doped materials [24, 25].

To see if there is a neutron spin resonance mode in underdoped $\text{BaFe}_{1.925}\text{Ni}_{0.075}\text{As}_2$ and to compare its c -axis dispersion with optimally doped $\text{BaFe}_{1.9}\text{Ni}_{0.1}\text{As}_2$ [21], we carried out constant- Q scans at $Q = (0.5, 0.5, 0)$ and $(0.5, 0.5, 1)$ above and below the superconducting transition temperature T_c . Figure 2(a) shows the raw data collected on the HB-3 triple-axis spectrometer at the signal $Q = (0.5, 0.5, 0)$ and background $Q = (0.7, 0.7, 0)$ positions. There is clear intensity gain at $Q = (0.5, 0.5, 0)$ near $E = 7 \text{ meV}$ below T_c at the expense of spectral weight loss below $\sim 4 \text{ meV}$. The temperature difference spectrum between 2 K and 20 K in Fig. 2(b) confirms the presence of the mode at $E = 7 \text{ meV}$ below T_c and a reduction in spectral weight below 4 meV . The open squares in Fig. 2(a) show the energy dependence of the background scattering at $Q = (0.7, 0.7, 0)$.

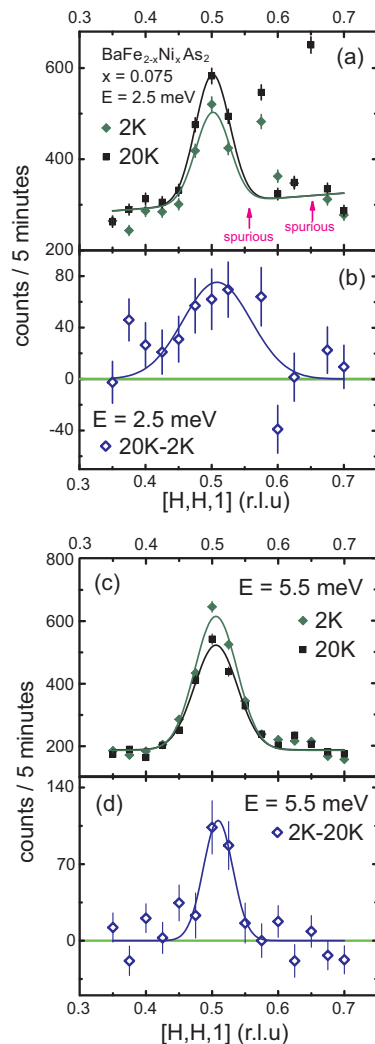


FIG. 5. (color online) (a) Q -scans along the $(H, H, 1)$ direction at $E = 2.5 \text{ meV}$ above and below T_c for $\text{BaFe}_{1.925}\text{Ni}_{0.075}\text{As}_2$. (b) Temperature difference plot shows that the scattering at $Q = (0.5, 0.5, 1)$ and $E = 2.5 \text{ meV}$ decreases below T_c . (c) Identical Q -scans across T_c at the resonance energy of $E = 5.5 \text{ meV}$. The scattering enhances below T_c . (d) Temperature difference plot between 2 K and 20 K, showing clear field-induced scattering below T_c at $Q = (0.5, 0.5, 1)$.

Figures 3 summarizes constant-energy scans at $E = 7 \text{ meV}$ and 3 meV along the $[H, H, 0]$ direction. At the resonance energy, the scattering shows a well-defined peak centered at $Q = (0.5, 0.5, 0)$ that increases in intensity below T_c [Fig. 3(a)]. Figure 3(b) shows the temperature difference plot which confirms that the intensity gain below T_c in Fig. 2(a) occurs at $Q = (0.5, 0.5, 0)$. Similarly, constant-energy scans at $E = 3 \text{ meV}$ above and below T_c in Fig. 3(c) reveal clear normal state magnetic scattering that is not completely suppressed (gapped) below T_c , at least with the energy resolution afforded with these thermal triple-axis measurements. Figure 2(c) shows our esti-

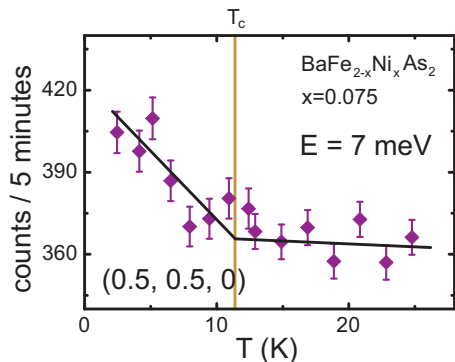


FIG. 6. (color online) (a) Temperature dependence of the $E = 7$ meV scattering at $Q = (0.5, 0.5, 0)$ for $\text{BaFe}_{1.925}\text{Ni}_{0.075}\text{As}_2$. The scattering increases in intensity below T_c of 12.3 K.

mation of the energy dependence of the dynamic susceptibility $\chi''(Q, \omega)$ above and below T_c , obtained by subtracting the background and correcting for the Bose population factor using $\chi''(Q, \omega) = [1 - \exp(-\hbar\omega/k_B T)]S(Q, \omega)$, where $E = \hbar\omega$. While the normal state susceptibility appears to increase linearly with energy, superconductivity rearranges the spectrum, creating a (pseudo) spin gap below 4 meV and a neutron spin resonance at $E = 7$ meV for in-phase spin fluctuations along the c -axis ($L = 0$).

To investigate the behavior for the out-of-phase spin fluctuations along the c -axis, we plot in Fig. 4(a) constant- Q scans at $Q = (0.5, 0.5, 1)$ above and below T_c . Figure 4(b) shows the temperature difference plot, and a comparison of Fig. 4(b) and Fig. 2(b) immediately reveals that the neutron spin resonance has moved from $E = 7$ meV at $Q = (0.5, 0.5, 0)$ to $E = 5$ meV at $Q = (0.5, 0.5, 1)$. Note in particular that for $Q = (0.5, 0.5, 0)$ there is essentially no change with temperature for the scattering at 5 meV (Fig. 2), which is where the maximum in intensity occurs at the $Q = (0.5, 0.5, 1)$ position. This is compelling evidence that the neutron spin resonance is dispersive for both underdoped and optimally doped $\text{BaFe}_{2-x}\text{Ni}_x\text{As}_2$.

Figure 5 shows constant-energy scans along the $[H, H, 1]$ direction and the temperature difference data between 2 K and 20 K for $E = 2.5, 5.5$ meV. Similar to the $[H, H, 0]$ scans in Fig. 3, we find that superconductivity only reduces but does not completely suppress the magnetic scattering at $E = 2.5$ meV [Figs. 5(a) and 5(b)]. Similarly, the scattering near the resonance energy at $E = 5.5$ meV shows a clear increase below T_c . To test if the intensity gain at $E = 7$ and $Q = (0.5, 0.5, 0)$ is responding to superconductivity, we show in Fig. 6 the temperature dependence of the scattering, which clearly increases below T_c consistent with the temperature dependence of the neutron spin resonance [19–22, 24–26].

To determine the c -axis modulation of the spin excitations at different temperatures and energies, we show

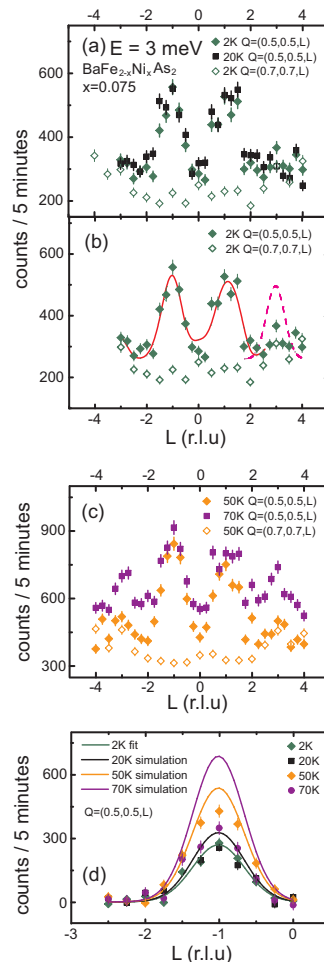


FIG. 7. (color online) Constant-energy scans along the $(0.5, 0.5, L)$ (signal) and $(0.7, 0.7, L)$ (background) directions at $E = 3$ meV and various temperatures. (a) The scattering at 2 K and 20 K shows well-defined peaks centered at $L = \pm 1$. Fourier transform of these peaks give c -axis spin-spin correlation length of ~ 14 Å. (b) Signal and background Scattering at 2 K. The solid line is Gaussian fits to the data. The dashed line shows the expected magnetic scattering at $Q = (0.5, 0.5, 3)$ assuming Fe^{2+} form factor. The absence of clear peaks at $L = \pm 3$ suggests that magnetic scattering in $\text{BaFe}_{1.925}\text{Ni}_{0.075}\text{As}_2$ damps out much faster than expected. (c) Similar scans at 50 K and 70 K. (d) The solid lines in the Figure show the effect of Bose population factor as a function of increasing temperature if one normalizes the magnetic scattering above background at 2 K. The magnetic intensity changes in the system clearly does not obey the Bose statistics, indicating that the scattering is not spin waves.

in Figs. 7, 8, and 9 constant-energy scans along the $Q = (0.5, 0.5, L)$ (signal) and $Q = (0.7, 0.7, L)$ (background) directions at $E = 3, 5.5,$ and 7 meV, respectively. Inspection of the data immediately suggests that the scattering is antiferromagnetically correlated between the layers along the c -axis. To model the AF spin correlations along the c -axis, we assume their structure factor is

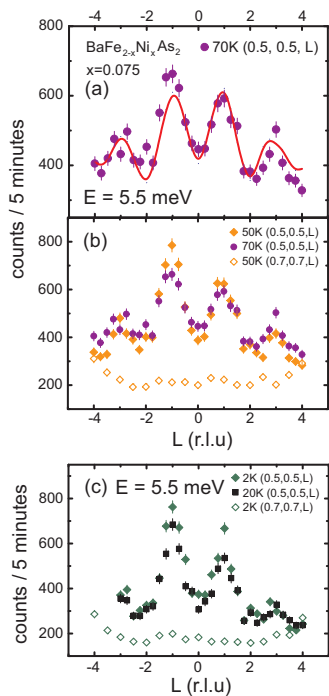


FIG. 8. (color online) Constant-energy scans along the $(0.5, 0.5, L)$ (signal) and $(0.7, 0.7, L)$ (background) directions at the resonance energy of $E = 5.5$ meV and various temperatures. (a) The c -axis scattering at 70 K. (b) The signal and background scattering at 50 K. The data again show clear peaks at $L = \pm 1$ but much damped peaks at $L = \pm 3$. (c) Signal and background scattering at 2 K and 20 K. Superconductivity clearly enhances magnetic scattering at $L = 0$ and $L = \pm 1$. The spin-spin correlation length is again about 14 Å and is weakly temperature dependent in the probed temperature range (2 K to 70 K).

similar to that of [42]: $f(Q_z) = F^2(Q)[S_0 + S_1 \exp(-(L - L_0)^2/2\sigma^2)]$, where $F(Q)$ is the magnetic form factor [43], $L = Q_z c/2\pi$, $L_0 = \pm 1, \pm 3, \dots$, σ is the width of the Gaussian which gives the correlation length of the spin excitations along the c -axis, S_0 and S_1 are fitting parameters for constant magnetic rod scattering along any L and maximum magnetic intensity at odd values of L , respectively.

Figure 7 shows the temperature dependence of the magnetic scattering at $E = 3$ meV along the c -axis. Starting from 2 K and 20 K in Fig. 7(a), we see two clear peaks centered around $Q = (0.5, 0.5, 1)$ and $(0.5, 0.5, -1)$ above the background. Gaussian fits to these peaks give a c -axis spin correlation length of ~ 14 Å [Fig. 7(b)]. Upon increasing temperature to 50 K and 70 K, the magnetic peaks at $Q = (0.5, 0.5, 1)$ and $(0.5, 0.5, -1)$ reduce in intensity but the c -axis spin-spin correlations appear not to be affected [Fig. 7(c)]. To test if the magnetic scattering below T_N simply follows the Bose population factor as expected for simple spin waves excitations, we show in Fig. 7(d) the temperature dependence of the mag-

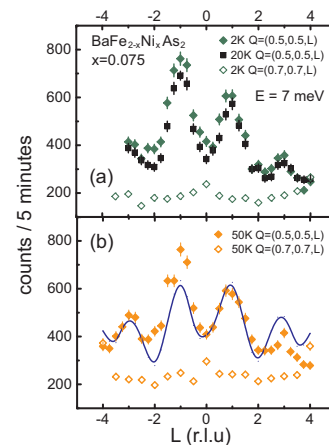


FIG. 9. (color online) L -dependence of the magnetic scattering for $\text{BaFe}_{1.925}\text{Ni}_{0.075}\text{As}_2$. (a) Identical scans as Fig. 8 except we now change the excitation energy to $E = 7$ meV. Comparison of the 2 K and 20 K data here indicates that the magnetic scattering below T_c at $L = 0$ is larger than that at $L = 1$. (b) Signal and background scattering at 50 K. The solid line shows the expected L -dependence of the magnetic scattering assuming simple Fe^{2+} form factor, which clearly fails to describe the data.

netic scattering normalized to the scattering at 2 K. The observed magnetic scattering clearly does not obey the Bose population factor, suggesting that the spin excitations in the doped materials are not simple spin waves, in contrast to the (undoped) parent compounds.

To probe the L -dependence of the magnetic scattering at the neutron spin resonance energies, we show in Figs. 8 and 9 constant-energy scans at $E = 5.5$ meV and 7 meV, respectively. Consistent with constant-energy scan data at $E = 3$ meV (Fig. 7), the magnetic scattering is still centered at $L = \pm 1, \pm 3$ positions and superconductivity has a relatively small effect on the overall magnetic scattering. Comparison of Figs. 2, 4, and 8, 9 reveals that the neutron spin resonance so clearly illustrated in the temperature difference scattering is a rather subtle effect that occurs at both $L = 0$ and $L = 1$ [Figs. 8(c) and 9(a)]. On warming to 50 K and 70 K, the magnetic scattering decreases but the c -axis spin correlation length of ~ 14 Å appears to be fairly temperature independent. The solid lines in Fig. 8(a) and 9(b) show Gaussian fits to the data which indicates that the decrease in the magnetic scattering along the c -axis direction falls off faster than just the Fe^{2+} form factor [43]. If we assume that the spins prefer to lie in the a - b plane as is the case for the AF undoped system, an additional reduction in intensity is expected due to the neutron spin-Fe-spin orientation factor and this brings the curve in reasonable agreement with the data. This result provides good evidence that the spins prefer to lie within the tetragonal a - b plane even in superconducting samples.

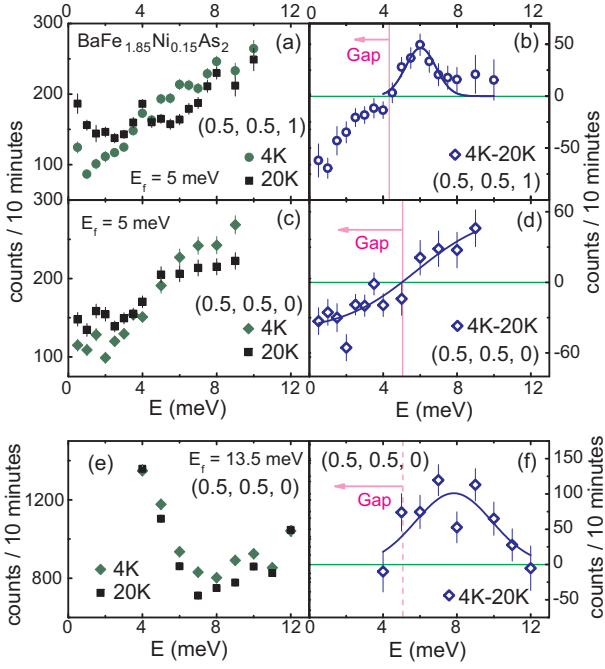


FIG. 10. (color online) Summary of constant- Q scans at various temperatures for $\text{BaFe}_{1.85}\text{Ni}_{0.15}\text{As}_2$ with $E_f = 5$ meV and 13.5 meV. (a) Energy dependence of scattering at $Q = (0.5, 0.5, 1)$ above and below T_c . The scattering shows a clear drop in intensity below $E = 4$ meV and enhancement near $E = 5$ meV. These data suggest that the effect of superconductivity is to open a low-energy spin gap and form a neutron spin resonance at $E = 5$ meV. (b) The temperature difference data confirm the formation of the neutron spin resonance. (c) Energy dependence of the scattering above and below T_c , now at $Q = (0.5, 0.5, 0)$. One can only probe magnetic scattering below $E = 9$ meV due to kinematic constraints with $E_f = 5$ meV. The scattering shows clear enhancement below T_c at energies around $E = 8$ meV, as confirmed by the temperature difference plot in (d). (e) Identical scan as that of (c) except we used $E_f = 13.5$ meV. Superconductivity induced neutron spin resonance can now be seen around $E = 8$ meV. (f) The temperature difference plot confirms the presence of the resonance at $E = 8$ meV.

Having described our comprehensive measurements on the underdoped $\text{BaFe}_{1.925}\text{Ni}_{0.075}\text{As}_2$, we now discuss inelastic neutron scattering experiments on the overdoped $\text{BaFe}_{1.85}\text{Ni}_{0.15}\text{As}_2$ [Figs. 1(a), 1(c)], where the static AF order is completely suppressed. These measurements were carried out on the PANDA cold triple-axis spectrometer. Figure 10 summarizes the constant- Q scans at $Q = (0.5, 0.5, 1)$ and $(0.5, 0.5, 0)$ below and above T_c . Using $E_f = 5$ meV, we find in Figs. 10(a) and 10(b) that the neutron spin resonance occurs at $E = 6$ meV for $Q = (0.5, 0.5, 1)$. Similar scans at $Q = (0.5, 0.5, 0)$ reveal clear scattering intensity enhancement above $E = 5$ meV [Figs. 10(c) and 10(d)]. However, kinematic constraints with the $E_f = 5$ meV spectrometer configuration did not allow a conclusive determination of the resonance

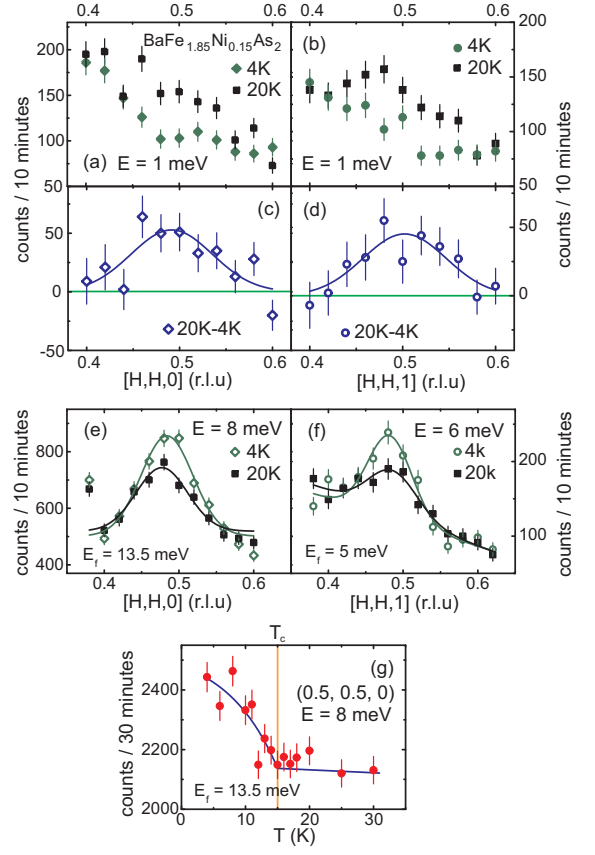


FIG. 11. (color online) Summary of constant-energy scans at an energy below the spin gap energy and at the resonance energy below and above T_c . (a) Q -scan along the $[H, H, 0]$ direction below and above T_c at $E = 1$ meV. There is a clear peak centered at $(0.5, 0.5, 0)$ that disappears below T_c , thus suggesting the opening of a clean spin-gap at $E = 1$ meV and $(0.5, 0.5, 0)$. (b) Similar scan along the $[H, H, 1]$ direction, again indicating the opening a spin gap at $E = 1$ meV and $(0.5, 0.5, 1)$. (c,d) Temperature difference plots confirm that superconductivity-induced spin gaps occur at $(0.5, 0.5, 0)$ and $(0.5, 0.5, 1)$ positions. (e) Constant-energy scans along the $[H, H, 0]$ direction below and above T_c at the resonance energy of $E = 8$ meV. (f) Similar scans at $E = 6$ meV along the $[H, H, 1]$ direction. In both cases, we find that superconductivity-induced changes happen at the expected wave-vectors. (g) Temperature dependence of the scattering at $E = 8$ meV and $Q = (0.5, 0.5, 0)$. The data show clear order-parameter-like increase below T_c , a hall mark of the neutron spin resonance.

energy. Figure 10(e) shows identical scans carried out with $E_f = 13.5$ meV. Inspection of Figs. 10(e) and 10(f) indicates that the resonance energy at $Q = (0.5, 0.5, 0)$ is now shifted to $E = 8$ meV. If we assume that the negative scattering in the temperature difference spectra of Figs. 10(b) and 10(d) gives the onset of the spin gap (assuming background scattering is temperature independent between 2 K and 20 K), these results suggest that the spin gap at $Q = (0.5, 0.5, 0)$ is larger than that at

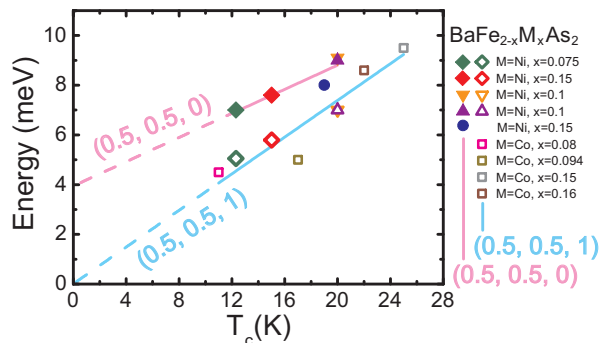


FIG. 12. (color online) Summary of electron-doping dependence of the neutron spin resonance energies at $Q = (0.5, 0.5, 0)$ and $(0.5, 0.5, 1)$ as a function of T_c . The data for $\text{BaFe}_{2-x}\text{Ni}_x\text{As}_2$ were from Refs. [21, 22, 41, 44] and present work. The data for $\text{BaFe}_{2-x}\text{Ni}_x\text{As}_2$ were from Refs. [20, 24–26]. The solid lines are linear fits to the data.

$Q = (0.5, 0.5, 1)$, consistent with the previous conclusions [22].

To determine if the low-energy spin excitations have a clean spin gap like those of the optimally doped $\text{BaFe}_{1.9}\text{Ni}_{0.1}\text{As}_2$ [21, 22], we took constant-energy scans along the $[H, H, 0]$ and $[H, H, 1]$ directions above and below T_c for $E = 1$ meV. Figures 11(a) and 11(b) show that spin excitations of $\text{BaFe}_{1.85}\text{Ni}_{0.15}\text{As}_2$ are gapless in the normal state for both $L = 0$ and 1 rlu, but open a clean gap below T_c at $E = 1$ meV. These results are similar to the optimally Ni-doped material, but are clearly different from underdoped $\text{BaFe}_{1.925}\text{Ni}_{0.075}\text{As}_2$ where there are no clean spin gap at $E = 2.5$ meV [Fig. 5(a)]. Figures 11(e) and 11(f) show wave-vector scans at the expected resonance energies for $Q = (0.5, 0.5, 0)$ and $(0.5, 0.5, 1)$. In both cases, we find clear intensity enhancement below T_c . The temperature dependent scattering at $Q = (0.5, 0.5, 0)$ and $E = 8$ meV in Fig. 11(g) shows clear order-parameter-like intensity increase below T_c , thus confirming the neutron spin resonance [19–22, 24–26].

Finally, we summarize in Figure 12 the electron-doping dependence of the neutron spin resonance at $Q = (0.5, 0.5, 0)$ and $(0.5, 0.5, 1)$ as a function of T_c for both $\text{BaFe}_{2-x}\text{Ni}_x\text{As}_2$ [21, 22, 41, 44] and $\text{BaFe}_{2-x}\text{Co}_x\text{As}_2$ [20, 24–26]. For copper oxide high- T_c superconductors, one of the hallmarks of the resonance is that its energy is proportional to T_c over a very wide temperature range [31, 32]. Since $\text{BaFe}_{2-x}\text{Ni}_x\text{As}_2$ has two resonances at distinctively different energies, its dispersion along the c -axis is related to the superconducting gap Δ_0 and its deviation δ via $E(Q_z) \sim 2\Delta_0 - 2\delta |\sin(Q_z/2)|$ [21]. The observation of a linear relationship for both mode energies and T_c suggests that $\delta/\Delta_0 = [\omega(0.5, 0.5, 0) - \omega(0.5, 0.5, 1)]/\omega(0.5, 0.5, 0)$ is approximately 0.28 and weakly Ni-doping dependent.

Therefore, the ratio of interplane (J_\perp) and intraplane (J_\parallel) AF coupling, J_\perp/J_\parallel , is weakly electron-doping dependent assuming that the values of Δ_0 and δ are proportional to J_\parallel and J_\perp , respectively.

We now discuss the physical interpretation of the above results. In the theory of spin-fluctuation-mediated superconductivity [9–13], the electron pairing arises from sign-reversed S -wave interband scattering between hole pockets centered at the Γ point and electron pockets at the M points [inset in Fig. 1(a)] [15–18]. One of the consequences of such electron-hole pocket excitations is to induce a resonance peak at the AF ordering wave vector $Q = (0.5, 0.5, 0)$ in the spin excitations spectrum. In the strictly two-dimensional model, the energy of the resonance is at (or slightly less than) the addition of hole (Δ_0^h) and electron (Δ_0^e) superconducting gap energies ($\Delta_0 = \Delta_0^h + \Delta_0^e$). Our previous finding of three-dimensionality of the resonance in optimally doped $\text{BaFe}_{1.9}\text{Ni}_{0.1}\text{As}_2$ [21, 22] suggests that the superconducting gap energy Δ_0 should be three-dimensional as well and sensitive on the Q values along the c -axis. The new results reported in the present paper on underdoped $\text{BaFe}_{1.925}\text{Ni}_{0.075}\text{As}_2$ and overdoped $\text{BaFe}_{1.85}\text{Ni}_{0.15}\text{As}_2$ confirm the earlier conclusion, and reveal that the three-dimensional nature of the superconducting gap is prevalent throughout the superconducting dome. If spin excitations are mediating the electron pairing for superconductivity, these results would suggest that the AF exchange coupling along the c -axis (J_\perp) contributes significantly to the electron pairing. Although the overall spin excitations as a function of increasing electron doping transform into quasi two-dimensional spin excitations rather rapidly as demonstrated by the disappearing anisotropic spin gaps at $Q = (0.5, 0.5, 0)$ and $(0.5, 0.5, 1)$ with increasing Ni-doping [41], the superconductivity-induced resonance retains its three-dimensional character even in the overdoped regime. This means that the superconducting electronic gaps in the iron-arsenic based materials are three-dimensional and quite different from that of the copper oxide superconductors.

IV. CONCLUSIONS

In summary, we have determined the doping evolution of the low-energy spin excitations in $\text{BaFe}_{2-x}\text{Ni}_x\text{As}_2$ for both underdoped and overdoped superconductors. In underdoped $\text{BaFe}_{1.925}\text{Ni}_{0.075}\text{As}_2$ we find that the appearance of bulk superconductivity is associated with the appearance of a weak three-dimensional neutron spin resonance. The spectral weight gain of the resonance below T_c is a rather small portion of the overall normal state magnetic scattering, and is compensated by opening a weak pseudo spin gap and reduction in static magnetic moment. Our Ni-doping dependent investigation of the spin gap and neutron spin resonance reveals that

the three-dimensional nature of the mode found earlier for the optimally doped sample is a universal property of Ni-doped superconductors. These results in turn suggest that AF spin excitations between the layers are also important for the superconductivity of these materials.

V. ACKNOWLEDGEMENTS

We thank Jiangping Hu and Tao Xiang for helpful discussions. The neutron scattering part of this work at UT/ORNL is supported by the U.S. NSF No. DMR-0756568, and by the U.S. DOE, Division of Scientific User Facilities. The single crystal growth effort at UT is supported by U.S. DOE BES No. DE-FG02-05ER46202. The single crystal growth and neutron scattering work at IOP is supported by Chinese Academy of Sciences and 973 Program (2010CB833102).

* slli@aphy.iphys.ac.cn

† daip@ornl.gov

- [1] Y. Kamihara, T. Watanabe, M. Hirano, and H. Hosono, *J. Am. Chem. Soc.* **130**, 3296 (2008).
- [2] M. Rotter, M. Tegel, and D. Johrendt, *Phys. Rev. Lett.* **101**, 107006 (2008).
- [3] L. J. Li, Y. K. Luo, Q. B. Wang, H. Chen, Z. Ren, Q. Tao, Y. K. Li, X. Lin, M. He, Z. W. Zhu, G. H. Cao, and Z. A. Xu, *New. J. Phys.* **11**, 025008 (2009).
- [4] S. L. Bud'ko, N. Ni, and P. C. Canfield, *Phys. Rev. B* **79**, 220516(R) (2009).
- [5] C. de la Cruz, Q. Huang, J. W. Lynn, J. Li, W. Ratcliff II, J. L. Zarestky, H. A. Mook, G. F. Chen, J. L. Luo, N. L. Wang, Pengcheng Dai, *Nature (London)* **453**, 899 (2008).
- [6] Jun Zhao, Q. Huang, C. de la Cruz, Shiliang Li, J. W. Lynn, Y. Chen, M. A. Green, G. F. Chen, G. Li, Z. Li, J. L. Luo, N. L. Wang, Pengcheng Dai, *Nature Materials* **7**, 953 (2008).
- [7] Q. Huang, Y. Qiu, Wei Bao, J.W. Lynn, M.A. Green, Y. Chen, T. Wu, G. Wu, X.H. Chen, *Phys. Rev. Lett.* **101**, 257003 (2008).
- [8] Jun Zhao, W. Ratcliff II, J. W. Lynn, G. F. Chen, J. L. Luo, N. L. Wang, J. Hu, Pengcheng Dai, *Phys. Rev. B* **78**, 140504(R) (2008).
- [9] I. I. Mazin, D. J. Singh, M. D. Johannes, and M. H. Du, *Phys. Rev. Lett.* **101**, 057003 (2008).
- [10] A. V. Chubukov, *Physica C* **469**, 640 (2009).
- [11] F. Wang, H. Zhai, Y. Ran, A. Vishwanath, and D.-H. Lee, *Phys. Rev. Lett.* **102**, 047005 (2009).
- [12] V. Cvetkovic and Z. Tesanovic, *Eur. Phys. J. Lett.* **85**, (2009).
- [13] A. Moreo, M. Daghofer, J. A. Riera, and E. Dagotto, *Phys. Rev. B* **79**, 134502 (2009).
- [14] I. I. Mazin and J. Schmalian, *Physica C* **469**, 614 (2009).
- [15] T. A. Maier and D. J. Scalapino, *Phys. Rev. B* **78**, 020514(R) (2008).
- [16] T. A. Maier, S. Graser, D. J. Scalapino, and P. Hirschfeld, *Phys. Rev. B* **79**, 134520 (2009).
- [17] M. M. Korshunov and I. Eremin, *Phys. Rev. B* **78**, 140509(R) (2008).
- [18] Kangjun Seo, Chen Fang, B. Andrei Bernevig, and Jiangping Hu, *Phys. Rev. B* **79**, 235207 (2009).
- [19] A. D. Christianson, E. A. Goremychkin, R. Osborn, S. Rosenkranz, M. D. Lumsden, C. D. Malliakas, I. S. Todorov, H. Claus, D. Y. Chung, M. G. Kanatzidis, R. I. Bewley and T. Guidi, *Nature (London)* **456**, 930 (2008).
- [20] M. D. Lumsden, A. D. Christianson, D. Parshall, M. B. Stone, S. E. Nagler, G. J. MacDougall, H. A. Mook, K. Lokshin, T. Egami, D. L. Abernathy, E. A. Goremychkin, R. Osborn, M. A. McGuire, A. S. Sefat, R. Jin, B. C. Sales, and D. Mandrus, *Phys. Rev. Lett.* **102**, 107005 (2009).
- [21] Songxue Chi, Astrid Schneidewind, Jun Zhao, Leland W. Harriger, Linjun Li, Yongkang Luo, Guanghan Cao, Zhuan Xu, Micheal Loewenhaupt, Jiangping Hu, and Pengcheng Dai, *Phys. Rev. Lett.* **102**, 107006 (2009).
- [22] Shiliang Li, Ying Chen, Sung Chang, Jeffrey W. Lynn, Linjun Li, Yongkang Luo, Guanghan Cao, Zhuan Xu, and Pengcheng Dai *Phys. Rev. B* **79**, 174527 (2009).
- [23] D. Parshall, K. A. Lokshin, Jennifer Niedziela, A. D. Christianson, M. D. Lumsden, H. A. Mook, S. E. Nagler, M. A. McGuire, M. B. Stone, D. L. Abernathy, A. S. Sefat, B. C. Sales, D. G. Mandrus, and T. Egami, *Phys. Rev. B* **80**, 012502 (2009).
- [24] D. K. Pratt, W. Tian, A. Kreyssig, J. L. Zarestky, S. Nandi, N. Ni, S. L. Budko, P. C. Canfield, A. I. Goldman, and R. J. McQueeney, *Phys. Rev. Lett.* **103**, 087001 (2009).
- [25] A. D. Christianson, M. D. Lumsden, S. E. Nagler, G. J. MacDougall, M. A. McGuire, A. S. Sefat, R. Jin, B. C. Sales, and D. Mandrus, *Phys. Rev. Lett.* **103**, 087002 (2009).
- [26] D. S. Inosov, J. T. Park, P. Bourges, D. L. Sun, Y. Sidis, A. Schneidewind, K. Hradil, D. Haug, C. T. Lin, B. Keimer and V. Hinkov, doi:10.1038/nphys1483.
- [27] J. Rossat-Mignod, L. P. Regnault, C. Vettier, P. Bourges, P. Bulet, J. Bossy, J. Y. Henry, and G. Lapertot, *Physica C (Amsterdam)* **185**, 86 (1991).
- [28] Pengcheng Dai, H. A. Mook, R. D. Hunt, and F. Doğan, *Phys. Rev. B* **63**, 054525 (2001).
- [29] H. F. Fong, B. Keimer, D. Reznik, D. L. Milius, and I. A. Aksay, *Phys. Rev. B* **54**, 6708 (1996).
- [30] C. Stock, W. J. L. Buyers, R. Liang, D. Peets, Z. Tun, D. Bonn, W. N. Hardy, and R. J. Birgeneau, *Phys. Rev. B* **69**, 014502 (2004).
- [31] Stephen D. Wilson, Pengcheng Dai, Shiliang Li, Songxue Chi, H. J. Kang, and J. W. Lynn, *Nature (London)* **442**, 59 (2006).
- [32] Jun Zhao, Pengcheng Dai, Shiliang Li, Paul G. Freeman, Y. Onose, Y. Tokura *Phys. Rev. Lett.* **99**, 017001 (2007)
- [33] Jun Zhao, Dao-Xin Yao, Shiliang Li, Tao Hong, Y. Chen, S. Chang, W. Ratcliff, II, J. W. Lynn, H. A. Mook, G. F. Chen, J. L. Luo, N. L. Wang, E. W. Carlson, Jiangping Hu, and Pengcheng Dai, *Phys. Rev. Lett.* **101**, 167203 (2008).
- [34] R. A. Ewings, T. G. Perring, R. I. Bewley, T. Guidi, M. J. Pitcher, D. R. Parker, S. J. Clarke, and A. T. Boothroyd, *Phys. Rev. B* **78**, 220501(R) (2008).
- [35] R. J. McQueeney, S. O. Diallo, V. P. Antropov, G. D. Samolyuk, C. Broholm, N. Ni, S. Nandi, M. Yethiraj, J. L. Zarestky, J. J. Pulikotil, A. Kreyssig, M. D. Lumsden, B. N. Harmon, P. C. Canfield, and A. I. Goldman, *Phys.*

- Rev. Lett. **101**, 227205 (2008).
- [36] K. Matan, R. Morinaga, K. Iida, and T. J. Sato, Phys. Rev. B **79**, 054526 (2009).
- [37] S. O. Diallo, V. P. Antropov, T. G. Perring, C. Broholm, J. J. Pulikkotil, N. Ni, S. L. Budko, P. C. Canfield, A. Kreyssig, A. I. Goldman, and R. J. McQueeney, Phys. Rev. Lett. **102**, 187206 (2009).
- [38] Jun Zhao, D. T. Adroja, Dao-Xin Yao, R. Bewley, Shiliang Li, X. F. Wang, G. Wu, X. H. Chen, Jiangping Hu and Pengcheng Dai, Nat. Phys. **5**, 555 (2009).
- [39] J.-H. Chu, J. G. Analytis, C. Kucharczyk, and I. R. Fisher, Phys. Rev. B **79**, 014506 (2008).
- [40] C. Lester, Jiun-Haw Chu, J. G. Analytis, S. C. Capelli, A. S. Erickson, C. L. Condon, M. F. Toney, I. R. Fisher, and S. M. Hayden, Phys. Rev. B **79**, 144523 (2009).
- [41] Leland W. Harriger, Astrid Schneidewind, Shiliang Li, Jun Zhao, Zhengcai Li, Wei Lu, Xiaoli Dong, Fang Zhou, Zhongxian Zhao, Jiangping Hu, and Pengcheng Dai, Phys. Rev. Lett. **103**, 087005 (2009).
- [42] S.O. Diallo, D.K. Pratt, R.M. Fernandes, W. Tian, J.L. Zarestky, M. Lumsden, T.G. Perring, C.L. Broholm, N. Ni, S.L. Bud'ko, P.C. Canfield, H.-F. Li, D. Vaknin, A. Kreyssig, A.I. Goldman, R.J. McQueeney, arXiv:1001.2804v1.
- [43] W. Ratcliff II, P. A. Kienzle, Jeffrey W. Lynn, Shiliang Li, Pengcheng Dai, G. F. Chen, N. L. Wang, arXiv:1001.1941.
- [44] Jun Zhao, Louis-Pierre Regnault, Chenglin Zhang, Miaoying Wang, Zhengcai Li, Fang Zhou, Zhongxian Zhao, Pengcheng Dai, arXiv:0908.0954.